ORIGINAL RESEARCH

Prognostic role of PET/MRI hybrid imaging in patients with pulmonary arterial hypertension

Remigiusz Kazimierczyk ,[1] Piotr Szumowski,[2,3] Stephan G Nekolla,[4] Piotr Blaszczak,[5] Lukasz A Malek,[6] Barbara Milosz-Wieczorek,[7] Jolanta Misko,[8] Dorota Jurgilewicz,[2,3] Marcin Hladunski,[2,3] Malgorzata Knapp,[1] Bozena Sobkowicz,[1] Janusz Mysliwiec,[2] Ryszard Grzywna,[5] Wlodzimierz J Musial,[1] Karol A Kaminski [1,9]

► Additional material is published online only. To view, please visit the journal online (http://dx.doi.org/10.1136/heartjnl-2020-316741).

For numbered affiliations see end of article.

Correspondence to
Professor Karol A Kaminski, Department of Population Medicine and Civilization Diseases Prevention, Medical University of Bialystok, ul. Waszyngtona 13a; Bialystok 15-276, Poland; fizklin@wp.pl

Received 18 February 2020
Revised 22 April 2020
Accepted 5 May 2020

To cite: Kazimierczyk R, Szumowski P, Nekolla SG, *et al*. *Heart* Epub ahead of print: [*please include* Day Month Year]. doi:10.1136/heartjnl-2020-316741

ABSTRACT

Objective Right ventricular (RV) function is a major determinant of survival in patients with pulmonary arterial hypertension (PAH). Metabolic alterations may precede haemodynamic and clinical deterioration. Increased RV fluorodeoxyglucose (FDG) uptake in positron emission tomography (PET) was recently associated with progressive RV dysfunction in MRI, but the prognostic value of their combination has not been established.

Methods Twenty-six clinically stable patients with PAH (49.9±15.2 years) and 12 healthy subjects (control group, 44.7±13.5 years) had simultaneous PET/MRI scans. FDG uptake was quantified as mean standardised uptake value (SUV) for both left ventricle (LV) and RV. Mean follow-up time of this study was 14.2±7.3 months and the clinical end point was defined as death or clinical deterioration.

Results Median SUV_{RV}/SUV_{LV} ratio was 1.02 (IQR 0.42–1.21) in PAH group and 0.16 (0.13–0.25) in controls, p<0.001. In PAH group, SUV_{RV}/SUV_{LV} significantly correlated with RV haemodynamic deterioration. In comparison to the stable ones, 12 patients who experienced clinical end point had significantly higher baseline SUV_{RV}/SUV_{LV} ratio (1.21 (IQR 0.87–1.95) vs 0.53 (0.24–1.08), p=0.01) and lower RV ejection fraction (RVEF) (37.9±5.2 vs 46.8±5.7, p=0.03). Cox regression revealed that SUV_{RV}/SUV_{LV} ratio was significantly associated with the time to clinical end point. Kaplan-Meier analysis showed that combination of RVEF from MRI and SUV_{RV}/SUV_{LV} assessment may help to predict prognosis.

Conclusions Increased RV glucose uptake in PET and decreased RVEF identify patients with PAH with worse prognosis. Combining parameters from PET and MRI may help to identify patients at higher risk who potentially benefit from therapy escalation, but this hypothesis requires prospective validation.

INTRODUCTION

Pulmonary arterial hypertension (PAH) is a progressive disease characterised by the remodelling of pulmonary vessels, leading to the increase in the pulmonary vascular resistance (PVR), right ventricular (RV) afterload and inevitably to the right ventricle failure.[1] The RV is not prepared to cope with several fold increase of PVR and therefore symptoms of decreased cardiac output (CO) and RV failure are common in this rapidly progressive disease.[2] The importance of maintaining RV function in PAH is further reflected by the prognostic significance of multiple haemodynamic and imaging parameters of RV function, including RV ejection fraction (RVEF) and CO, some of which are best assessed in MRI.[3–8] In normal conditions, almost 95% of energy in myocardium is derived from mitochondrial oxidative phosphorylation (predominantly from fatty acids and to lesser extent carbohydrate metabolism), with the remainder coming from glycolysis.[8] It was previously published that increased pulmonary arterial pressures are associated with higher ^{18}F-fluorodeoxyglucose (FDG) uptake in the right ventricle using positron emission tomography (PET) imaging.[9] It is an evidence of 'metabolic shift' occurring in cardiomyocytes due to pressure overload, and FDG uptake correlates with PAH progression and unfavourable outcomes.[10 11] The integrated hybrid design provides truly simultaneous PET and MRI with advantages for imaging of dynamic processes visualised on either PET or MRI.[12 13] Therefore, we hypothesised hybrid PET/MRI scans in patients diagnosed with PAH will elucidate the relationship between RV haemodynamic parameters (derived from MRI and right heart catheterisation (RHC)) and metabolic changes occurring in myocardium. The second aim of this hypothesis driven study was to investigate whether PET/MRI hybrid imaging could provide new prognostic parameters in patients with PAH.

MATERIALS AND METHODS

Population characteristics

We enrolled 26 clinically stable adult patients diagnosed with PAH (from two PAH expert centres in Poland—Bialystok and Lublin) between January and May 2016. The initial diagnosis of precapillary pulmonary hypertension (PH) was made based on right heart catheterisation (mean pulmonary artery pressure (mPAP) ≥25 mm Hg, pulmonary artery wedge pressure (PAWP) ≤15 mm Hg) and the use of an algorithm that included a perfusion lung scan, echocardiography, respiratory function tests and CT to rule out secondary PH causes according to European guidelines.[7] The exclusion criteria were the following: WHO functional class IV, Eisenmenger physiology, PAH associated with prevalent systemic-to-pulmonary shunts due to moderate-to-large

Table 1 Basic characteristics of pulmonary arterial hypertension (PAH) group and healthy controls

	PAH	Controls	P value
Subjects, n	26	12	
Age, years	49.7±15.2	44.7±13.5	0.26
Sex (females), % (n)	68 (17)	67 (8)	
6 min walking test distance, m	382±102.3		
BNP, pg/mL	78.8 (46–282)		
Idiopathic/heritable PAH, % (n)	65 (17)		
Connective tissue disease-related PAH, % (n)	15 (4)		
Congenital heart disease-related PAH, % (n)	20 (5)		
Phosphodiesterase type 5 inhibitors, % (n)	38 (10)		
Endothelin receptor antagonists, % (n)	11 (3)		
Prostacyclins, % (n)	20 (5)		
Phosphodiesterase type 5 inhibitors+endothelin receptor antagonists, % (n)	31 (8)		
Haemodynamics			
Systemic pulmonary artery pressure, mm Hg	79.6±30.7		
Diastolic pulmonary artery pressure, mm Hg	31.9±13.5		
Mean pulmonary artery pressure, mm Hg	48.9±18.7		
Pulmonary capillary wedge pressure, mm Hg	10.5±2.03		
Diastolic pulmonary gradient, mm Hg	21.8±13.1		
Pulmonary vascular resistance, Wood units	9.1±5.6		
Cardiac index, L/min/m^2	2.6±0.6		
Right atrium pressure, mm Hg	8.2±2.9		
RV parameters (MRI)			
RV ejection fraction, %	44.9±7.9	63.8±5.8	<0.001
RV EDV/BSA, mL/m^2	118.2±21.7	73.6±12.2	0.001
RV ESV/BSA, mL/m^2	65.9±20.3	28.2±9.6	<0.001
RV mass/BSA, g/m^2	38.8±13.9	23.8±4.9	<0.001
RV compacted myocardium thickness, mm	5.7±1.5	2.6±0.4	0.001
Pulmonary arterial compliance, mL/mm Hg	2.5±1.9		
Right ventricle stroke work index, g•m•m^2/beat	20.5±8.7		
Myocardial metabolism (PET)			
SUV_{RV}	3.3 (2.3–6.5)	0.8 (0.5–0.9)	<0.001
SUV_{LV}	4.6 (3.2–7.2)	3.1 (1.9–4.8)	0.04
SUV_{RV}/SUV_{LV} ratio	1.02 (0.42–1.21)	0.16 (0.13–0.25)	<0.001

Data presented as mean±SD (normal distribution; Student's t-test was used to compare two variables) or median (IQR) (non-normal distribution; Mann-Whitney U test was used to compare two variables).
BNP, B-type natriuretic peptide; BSA, body surface area; EDV, end-diastolic volume; ESV, end-systolic volume; LV, left ventricle; PET, positron emission tomography; RV, right ventricle; SUV, standardised uptake value.

defects (according to European guidelines),[7] group II, III, IV, V of PH, diagnosed diabetes mellitus and contraindications to cardiac MRI. The control group consisted of 12 healthy controls who were matched based on sex and age. During the baseline evaluation, we performed a physical examination, 6 min walk test, laboratory tests, for example, serum B-type natriuretic peptide (BNP), blood count and renal function parameters.

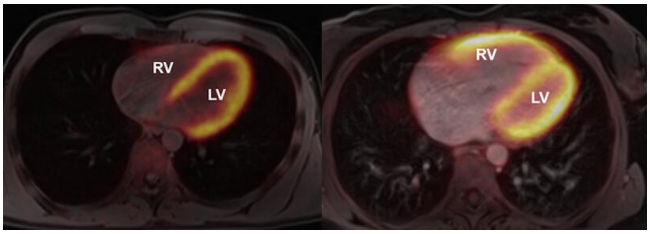

Figure 1 Left scan—PET/MRI scans of healthy control's heart (SUV_{RV} 0.3, SUV_{LV} 2.5). Right scan—patient's heart with highly elevated glucose uptake in RV wall in case of pulmonary arterial hypertension presence (SUV_{RV} 4.2, SUV_{LV} 3.1). LV, left ventricle; RV, right ventricle; SUV, standardised uptake value.

The clinical follow-up lasted 14.2±7.3 months. Death, WHO class worsening, hospitalisation due to PH progression or right heart failure were used as composite clinical end point (CEP) for Kaplan-Meier analysis. All enrolled patients were re-hospitalised in our Department and their clinical state was evaluated by PAH specialists (coauthors of this paper). PET/MRI results were not known to treating physician and did not affect the decision about the therapy.

This research was done without patient involvement in design, conduct, reporting or dissemination of the results.

Myocardial PET/MRI hybrid imaging

PET/MRI imaging was performed with a 3T Biograph mMR hybrid system (Siemens, Healthcare Erlangen, Germany) at the time of enrolment. Patients fasted overnight for at least 8 hours before myocardial PET imaging with a use of FDG as a tracer. The fasting blood glucose level was measured prior to the PET and patients were excluded from the study if their blood glucose level was >6.1 mmol/L (110 mg/dL). All patients were given Acipimox (niacin) 250 mg orally 1 hour before the PET and a carbohydrate-enriched and protein-enriched meal for glucose loading 2 hours before the injection of FDG.[14] One hour after intravenous injection of FDG (185 MBq±15 MBq), myocardial PET imaging was performed as previously described.[15]

For semi-quantitative analysis of FDG metabolism (syngo.via software, Siemens) in the myocardium, the standardised uptake value (SUV) was used. SUVs were calculated by normalising the obtained tissue radioactivity concentrations to body weight, injected dose and corrected for plasma glucose levels (the latter normalised to glucose level of 5 mmol/L). In order to minimise the effect of wall width in our study, we used the mean SUV with a fixed threshold (50%) value of the maximal activity within the right or left ventricle volume of interest (VOI). Then we calculated the right ventricle mean SUV to the left ventricle mean SUV ratio (SUV_{RV}/SUV_{LV} ratio).[10 13]

All electrocardiographic-gated cardiac MRI studies were performed during the same session with PET imaging and were analysed off-line in consensus by three experienced medical doctors (LM, BM-W, JM) using a dedicated workstation and software (Mass V.7.6, Medis, Leiden, The Netherlands). Scout images and electrocardiographic-gated breath-hold steady state free precession (SSFP) cine images in 2-chamber and 4-chamber views were registered to set up final short axis imaging planes. Systolic function assessment was based on SSFP short axis images from the tricuspid valve insertion point to the apex to encompass the entire RV. The imaging parameters were the following: field of view 360 mm, matrix 256×256, repetition time approximately

Table 2 Spearman's correlations between PET-derived and MRI/RHC-derived parameters

Correlation coefficient (r); p-value	SUV_{RV}	$SUV_{RV/LV}$	RVEF
6MWT	r=-0.3; p=0.11	r=−0.35; p=0.07	r=0.08; p=0.7
BNP	r=0.16; p=0.42	r=0.28; p=0.15	r=−0.24; p=0.23
RV thickness	r=0.4; p=0.04	r=0.51; p=0.004*	r=−0.6; p=0.001*
RVEF	r=−0.44; p=0.02*	r=−0.52; p=0.007*	
mPAP	r=0.8; p=0.000003*	r=0.77; p=0.000005*	r=−0.58; p=0.002*
PVR	r=0.72; p=0.001*	r=0.62; p=0.0007*	r=−0.64; p=0.0004*
PAC	r=−0.63; p=0.0006*	r=−0.6; p=0.001*	r=0.31; p=0.12
RVSWI	r=0.74; p=0.00002*	r=0.72; p=0.0002*	r=−0.42; p=0.02*

*P value significant (<0.05) after Benjamini-Hochberg correction.
BNP, B-type natriuretic peptide; LV, left ventricle; mPAP, mean pulmonary arterial hypertension; 6MWT, 6 min walk test distance; PAC, pulmonary arterial compliance; PVR, pulmonary vascular resistance; RV, right ventricle; RVEF, right ventricle ejection fraction; RVSWI, right ventricle stroke work index; SUV, standardised uptake value.

40.7 ms, echo time 1.49 ms, flip angle 50 degrees, slice thickness 6 mm, gap 1.2 mm, in-plane image resolution 1.4×1.4×6 mm^3, temporal resolution 25 phases per cardiac cycle. Short-axis SSFP cine images were initially previewed from the base to the apex in a cinematic mode; then endocardial and epicardial contours for RV end-diastole and end-systole were manually traced.

MRI/RHC haemodynamic parameters

Right heart catheterisation was repeated at enrolment in standard technique within median 4[2–6] days of PET/MRI scans using a balloon-tipped 7F Swan-Ganz catheter; CO was measured by thermodilution method; PVR was calculated with the formula PVR=(mPAP−PAWP)/CO and expressed in Wood units (WU). Pulmonary artery compliance (PAC) was obtained by the formula PAC=systolic volume (SV)/(systolic pulmonary artery pressure–diastolic pulmonary artery pressure)[5]; right ventricle stroke work index (RVSWI) was calculated from measurements during RHC using an equation RVSWI=(mPAP−right atrium pressure (RAP))×(cardiac index/heart rate)×0.0136.[6]

Statistical analysis

The distribution of the variables was checked using the Kolmogorov-Smirnov test. The data are expressed as a mean±SD or median (IQR) as appropriate. Statistical analysis was performed using Student's t-test or Mann-Whitney U test for continuous data depending on distribution. Spearman's correlation coefficient was used to examine the relationship between

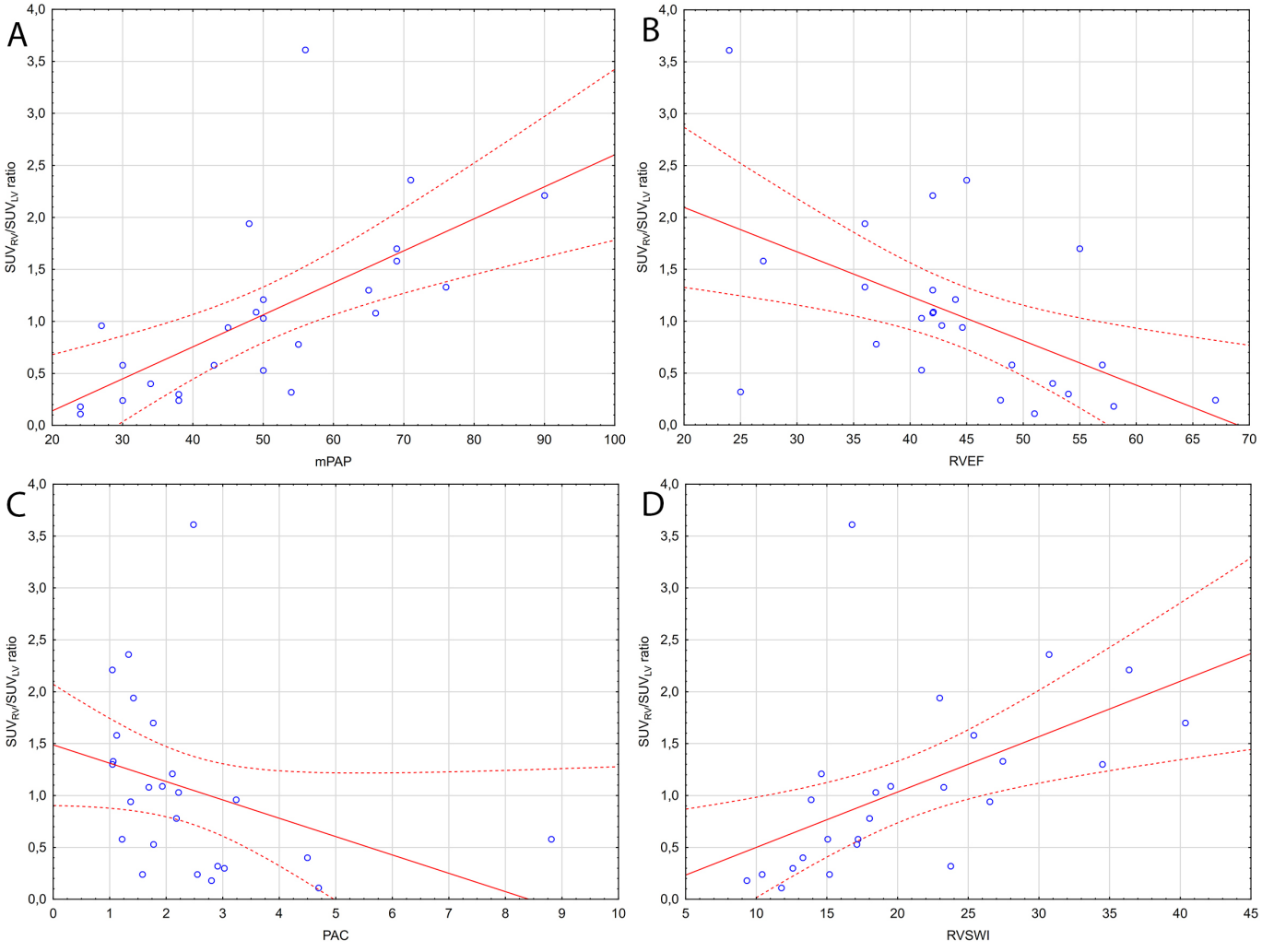

Figure 2 Spearman's correlations between mean SUV_{RV}/SUV_{LV} ratio and (A) mPAP (r=0.77, p=0.000005), (B) RVEF (r=−0.52, p=0.007), (C) PAC (r=−0.60, p=0.001), (D) RVSWI (r=0.72, p=0.0002). LV, left ventricle; PAC, pulmonary arterial compliance; mPAP, mean pulmonary artery pressure; RV, right ventricle; RVEF, RV ejection fraction; RVSWI, right ventricle stroke work index; SUV, standardised uptake value.

two continuous variables. Benjamini-Hochberg correction was used to account for multiple comparisons in correlation analysis. Univariable and multivariable Cox proportional hazards regression analyses were performed to identify independent variables associated with end point. Receiver operator characteristic curves (ROC) were plotted to determine the area under the curve (AUC) and sensitivity and specificity of the optimal cut-offs (binomial method). To investigate the occurrence of clinical end points, Kaplan-Meier method with log-rank test was implemented. P value <0.05 was deemed statistically significant. A statistical software package STATA V.13 (USA) was used for the analysis.

RESULTS

Patients' characteristics

The general characteristics of 26 patients with PAH (age 49.9±15.2 years, 17 females) is presented in the table 1. Five patients (19%) were incident cases while the rest of the study group were prevalent—receiving PAH-specific treatment at the time of survey. Most of them were in the WHO functional class III (61%, n=16) and 10 patients (39%) were in WHO functional class II. According to 1-year mortality risk groups presented in ESC guidelines,[7] 18 patients (69%) were at intermediate risk; 5 patients (19%) at low risk and 3 patients (12%) at high risk. Control group consisting of 12 healthy volunteers was selected based on age and sex.

PET/MRI parameters and RV function

In the PAH group, the glucose uptake in the RV, reported as the median standard uptake value (SUV_{RV}), was 3.3 (2.3–6.5); in left ventricle (SUV_{LV}) was 4.6 (3.2–7.2) and the mean SUV_{RV}/SUV_{LV} ratio was 1.02 (0.42–1.21). Both parameters were significantly higher than in the control group, where median SUV_{RV} was 0.8 (0.5–0.9); median SUV_{LV} was 3.1 (1.9–4.8) and the median SUV_{RV}/SUV_{LV} ratio was 0.16 (0.13–0.25). PET/MRI results are shown in table 1. Significant differences between higher RV glucose uptake in the study group indicates the presence of increased glucose consumption in PAH (figure 1). Increased glucose uptake in RV resulting in an elevated SUV_{RV}/SUV_{LV} ratio is closely associated with parameters of RV dysfunction and the ones depicting RV afterload (table 2, figure 2). Twelve patients (46%) had a ratio higher than 1 (RV glucose metabolism was higher than LV glucose metabolism), all of whom were in WHO class III. No associations between haemodynamic parameters of pulmonary circulation and FDG uptake in LV were observed.

Patients with moderate-to-severe PAH defined as mPAP ≥35 mm Hg derived from RHC[10] presented higher SUV_{RV}/SUV_{LV} ratio (1.21 (0.94–1.7) vs 0.27 (0.21–0.49), p=0.0004). There were also significant differences between other parameters like PVR and RVEF. Similarly, patients with impaired RV function in MRI (RVEF <40%) presented higher SUV_{RV}, SUV_{RV}/SUV_{LV} ratio and PVR than patients with RVEF >40% (online supplementary table S1).

Dividing PAH group on the basis of SUV_{RV}/SUV_{LV} ratio (higher and lower than 1, as in previous studies)[10] showed, that patients with higher glucose RV uptake than LV uptake had worse functional and haemodynamic parameters derived from MRI—RVEF, from RHC—CO, mPAP and PVR (table 3).

Composite end point results

Finally, we analysed PET/MRI parameters in subjects with PAH who had experienced clinical end point follow-up during 14.2±7.3 months (characteristics in table 4). Patients with clinical end point (46%, n=12, 2 deaths, 10 patients had clinical symptoms of PAH progression defined as WHO class worsening (3 patients) or hospitalisation due to symptoms of RV failure (7 patients)) presented statistically significant higher initial values of SUV_{RV} and SUV_{RV}/SUV_{LV} ratio than stable patients with no differences in mean SUV of left ventricle (table 4). Interestingly, two groups did not significantly differ in RHC-derived parameters—mPAP, CO or PVR. This could suggest that baseline changes in the RV metabolism may precede RV dysfunction expressed by well-established haemodynamic parameters.

Univariable Cox proportional hazard analysis showed that the WHO functional class, 6MWT distance, RAP, SUV_{RV} and SUV_{RV}/SUV_{LV} ratio were significantly associated with time to clinical end point. Multivariable Cox analysis demonstrated that the

Table 3 The comparison between patients with SUV_{RV}/SUV_{LV} ratio higher and lower than 1

	SUV_{RV}/SUV_{LV} ratio >1	SUV_{RV}/SUV_{LV} ratio <1	P value
Patients, n	12	14	
CO, L/min	4.1±0.7	5.4±1.0	0.003
mPAP, mm Hg	63.4±14.1	34.5±9.1	<0.001
DPG, mm Hg	31.4±10.1	12.2±7.4	0.003
RAP, mm Hg	9.4±2.9	7.0±2.5	0.04
RVEF, %	39.7±5.3	49.8±5.8	<0.001
PAC, mL/mm Hg	1.4±0.4	3.3±1.4	0.01
RVSWI, g×m×m^2/beat	25.3±7.0	14.7±4.6	0.01
PVR, Wood units	13.2±4.0	5.1±2.0	<0.001
BNP, pg/mL	255 (143–335)	55 (46–64)	0.07
6MWT distance, m	388.4±100.2	402.1±99.4	0.76

Data presented as mean±SD (normal distribution; Student's t-test was used to compare two variables) or median (IQR) (non-normal distribution; Mann-Whitney U test was used to compare two variables).
BNP, B-type natriuretic peptide; CO, cardiac output; DPG, diastolic pulmonary gradient; LV, left ventricle; mPAP, mean pulmonary artery pressure; 6MWD, 6 min walking test; PAC, pulmonary arterial compliance; PVR, pulmonary vascular resistance; RAP, right atrial pressure; RV, right ventricle; RVEF, right ventricle ejection fraction; RVSWI, right ventricle stroke work index.

Table 4 Comparison of patients with combined clinical end point and without clinical end point

	Clinical end point (+) patients	Clinical end point (–) patients	P value
Patients, n	12	14	
BNP, pg/mL	269 (99–481)	87 (46–258)	0.29
6MWT distance, m	364.9±92.5	443.6±71.4	0.09
SUV_{RV}	0.71 (0.38–1.04)	0.23 (0.16–0.59)	0.02
SUV_{LV}	0.65 (0.31–0.76)	0.63 (0.38–0.97)	0.68
SUV_{RV}/SUV_{LV} ratio	1.21 (0.87–1.95)	0.53 (0.24–1.08)	0.01
RVEF, %	37.9±5.2	46.8±5.7	0.03
PAC, mL/mm Hg	2.5±0.5	2.2±0.4	0.67
RVSWI, g•m•m^2/beat	22.8±8.9	18.4±7.6	0.18
mPAP, mm Hg	56.7±19.2	43.9±13.7	0.06
PVR, Wood units	10.7±5.1	7.7±3.1	0.24
RAP, mm Hg	10.7±3.9	6.7±0.2.7	0.009

Data presented as mean±SD (normal distribution; Student's t-test was used to compare two variables) or median (IQR) (non-normal distribution; Mann-Whitney U test was used to compare two variables).
BNP, B-type natriuretic peptide; CO, cardiac output; DPG, diastolic pulmonary gradient; LV, left ventricle; mPAP, mean pulmonary artery pressure; 6MWD, 6 min walking test; PAC, pulmonary arterial compliance; PVR, pulmonary vascular resistance; RAP, right atrial pressure; RV, right ventricle; RVEF, right ventricle ejection fraction; RVSWI, right ventricle stroke work index; SUV, standardised uptake value.

Table 5 Univariable and multivariable Cox proportional hazard analysis for the time to the end point

	Univariate Cox analysis			Multivariable Cox analysis*		
Value	**HR**	**95% CI**	**P value**	**HR**	**95% CI**	**P value**
WHO class	11.01	1.60 to 75.50	0.01	7.05	1.75 to 52.1	0.01
Age	1.01	0.96 to 1.06	0.57			
BSA	0.61	0.01 to 35.1	0.81			
BNP	1.1	0.91 to 1.11	0.30			
6MWT	0.98	0.96 to 0.99	0.01	0.98	0.96 to 0.99	0.01
PET parameters						
SUV_{LV}	0.3	0.02 to 3.57	0.35			
SUV_{RV}	14.3	1.1 to 185.1	0.04			
SUV_{RV}/SUV_{LV} ratio	5.25	1.08 to 25.4	0.03	3.62	1.57 to 8.37	0.002
MRI parameters						
LV EDV/BSA	0.98	0.94 to 1.02	0.39			
LV ESV/BSA	0.98	0.93 to 1.03	0.46			
LVEF	1.05	0.96 to 1.15	0.23			
LV mass/BSA	1.02	0.96 to 1.08	0.47			
RV EDV/BSA	1.0	0.98 to 1.03	0.47			
RV ESV/BSA	1.03	0.99 to 1.06	0.11			
RVEF	0.95	0.88 to 1.04	0.30			
RV mass/BSA	1.05	0.99 to 1.11	0.08			
PAC	1.09	0.70 to 1.45	0.09			
RVSWI	1.07	0.96 to 1.19	0.12			
RHC parameters						
mPAP	1.05	0.99 to 1.11	0.07			
PCWP	1.38	0.93 to 2.02	0.10			
DPG	1.07	0.99 to 1.14	0.06			
RAP	1.61	1.08 to 2.41	0.01	1.43	1.15 to 1.78	0.001
CI	0.47	0.11 to 1.95	0.30			
PVR	1.12	0.85 to 1.31	0.11			
SvO_2	1.02	0.91 to 1.15	0.34			

*Multivariable stepwise regression model included all univariate predictors, significance level of the model p<0.05.
BNP, B-type natriuretic peptide; BSA, body surface area; CI, cardiac index; DPG, diastolic pulmonary gradient; EDV, end-diastolic volume; ESV, end-systolic volume; LVEF, left ventricle ejection fraction; mPAP, mean pulmonary artery pressure; 6MWD, 6 min walking test distance; PAC, pulmonary arterial compliance; PAH, pulmonary arterial hypertension; PCWP, pulmonary capillary wedge pressure; PVR, pulmonary vascular resistance; RAP, right atrial pressure; RV, right ventricle; RVEF, right ventricle ejection fraction; RVSWI, right ventricle stroke work index; SUV, standardised uptake value; SvO_2, mixed venous oxygen saturation.

best model predicting time to clinical end point consisted of the SUV_{RV}/SUV_{LV} ratio, WHO functional class. 6MWT distance and RAP (table 5).

RVEF has been previously described as an important prognostic factor in PAH.[7] In our study, patients with RVEF <40% had worse prognosis, log-rank test p=0.03. Similarly, Kaplan-Meier curve showed worse prognosis for patients with SUV_{RV}/SUV_{LV}>1 (median value), log-rank test p=0.02. Simultaneous measurement of both: RVEF in MRI and SUV_{RV}/SUV_{LV} allowed comparison of prognosis of patients who presented both those unfavourable parameters, one or neither of them. Subgroup of patients with PAH with combined two conditions (RVEF <40% and SUV_{RV}/SUV_{LV}>1) had the worst prognosis, subjects with only one parameter better and ones without any the best survival rate (log-rank test, p=0.02, figure 3). Additionally, we used ROC curve analysis to determine cut-off values of RVEF—42% (AUC: 0.76 (0.56–0.96) and SUV_{RV}/SUV_{LV} 0.77 (AUC: 0.78 (0.6–0.96) for patients with clinical end point, online supplementary figure S1. When we divided patients with PAH into three groups based on the above-mentioned cut-offs obtained in ROC analysis (of RVEF 42% and SUV_{RV}/SUV_{LV} 0.77), we also observed statistically significant difference in survival between the groups (p=0.02, online supplementary figure S2).

Prevalent patients

We also repeated analysis of SUV_{RV}/SUV_{LV} prognostic utility in a subpopulation of 21 prevalent patients, whose prognosis differs from the incident patients. Similarly as in the whole population clinical end point (+) prevalent patients had a significantly higher SUV_{RV}/SUV_{LV} ratio than clinical end point (−) prevalent patients (1.19 (0.99–1.76) vs 0.57 (0.31–0.75), p=0.02) and cut-off value of SUV_{RV}/SUV_{LV} to predict clinical end point was 0.87 (AUC: 0.81, p=0.003). Also, in this subpopulation, patients with SUV_{RV}/SUV_{LV} >0.87 had significantly worse prognosis (log-rank test, p=0.03).

DISCUSSION

This is the first study to our knowledge that integrates metabolic PET imaging and MRI-derived haemodynamic parameters for the evaluation and prognosis of patients diagnosed with PAH using the PET/MRI hybrid.

The simultaneous PET/MRI imaging system is both novel and non-invasive diagnostic tool. PET is an excellent modern method that uses short-acting radiopharmaceutical that allows the molecular imaging to give insight on the intracellular metabolic processes in cells. The second component of this hybrid system, MRI, yields anatomical images with excellent quality.

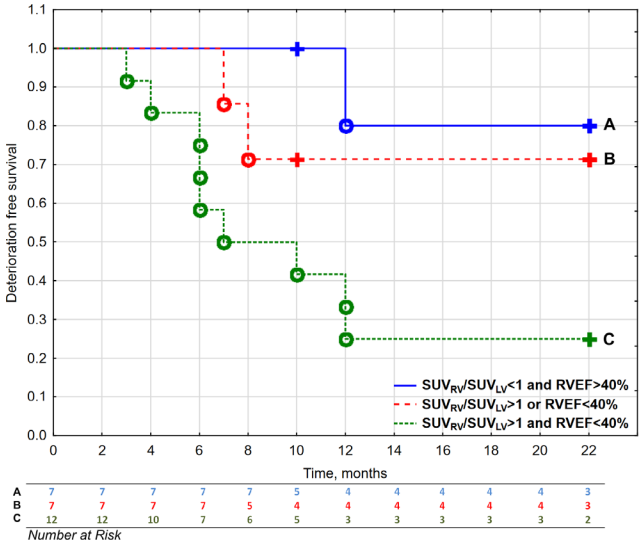

Figure 3 Kaplan-Meier curves presenting deterioration-free survival in patients with pulmonary arterial hypertension (PAH) based on $SUV_{RV/LV}$ ratio and RVEF, log-rank test, p=0.02. °, complete events; +, censored events; LV, left ventricle; RV, right ventricle; RVEF, RV ejection fraction; SUV, standardised uptake value.

Analysis of results of both modalities creating fusion images, especially when used with ECG gating, allows to indicate metabolic abnormalities in particular organs.[12]

Augmented PVR in PAH causes increased RV afterload that results in multiple adaptive changes including cardiomyocyte hypertrophy, chamber dilatation, increase in heart rate and RAP that sustain the CO. However, with the course of the disease these changes start maladaptive remodelling creating vicious circle of right heart failure. It is not clear what role changes of glucose metabolism in cardiomyocytes play in this phenomenon. In normal physiological conditions, cardiomyocytes use mainly fatty acid oxidation to produce energy. It changes in heart failure or during ischaemia. In an animal model of LV failure, a metabolic shift to glucose as primary energy substrate was noticed. It was associated with the extent of ventricular dysfunction and accompanying remodelling.[16–18] This fact is also reflected in our results since patients with PAH had significantly higher RV FDG uptake than the healthy controls. There is relatively little information available regarding the potential association between RV FDG uptake and the clinical status of patients with PAH. Tatebe *et al* suggested that a RV maximal SUV >8.3 was an independent predictor of clinical worsening in patients with PH after adjustment of WHO-FC, 6MWD or diastolic RV mass index.[19] In other study, RV FDG accumulation decreased after treatment with epoprostenol, proportionally to the degree of reduction in the PVR and RV peak-systolic wall stress.[20] Some researchers recently established that increased pulmonary arterial pressures are associated with an increase in the ratio of FDG uptake by RV and LV (SUV_{RV}/SUV_{LV}). Li *et al* showed that SUV_{RV}/SUV_{LV} ratios independently predicted mortality after adjusting for PVR, mean RAP and WHO functional class.[11] Furthermore, SUV_{RV}/SUV_{LV} ratio could independently predict RVEF after adjusted for age, body mass index, sex, mean RAP, mPAP and PVR.[21]

We found that increased glucose uptake in RV resulting in an elevated SUV_{RV}/SUV_{LV} ratio is closely associated with the presence of increased RV afterload, based on established haemodynamic parameters and linked to worse prognosis (similarly to previous results[9 10]). Moreover, parameters that depict RV dysfunction (RVSWI, RVEF) also correlated with RV glucose uptake.

Interestingly, correlations between SUV_{RV}/SUV_{LV} ratio and other established PAH prognostic factors—6MWT distance and serum BNP levels were not significant, suggesting that PET may provide additional prognostic information exceeding usually used risk scores. Patients enrolled in this study were stable, confirmed by relatively low BNP levels and distance of 6MWT (median 382 m). This may have influenced the relationship between metabolism and BNP, and what also observed in other small studies.[10] Moreover, in this respect we had relatively small within-group variability, what may impede finding statistical associations between these parameters.

Previous research have shown that PAC is linked with poorer prognosis in patients with PAH.[5] In our study, PAC strongly correlated with RV glucose consumption as depicted by FDG accumulation in SUV_{RV}/SUV_{LV} ratio. RVSWI is an important measure of RV function since it integrates standard haemodynamic parameters such as CO and has prognostic value in patients with PAH.[6] Similar to other parameters of RV overload, RVSWI correlated with metabolic shift in RV.

One of the problems of cardiac PET is the lack of established and widely accepted protocols on how one should measure SUV. In this study, we decided to use the method of calculating the mean SUV in the VOI defined by the 50% threshold as this is deemed less susceptible to partial volume effect,[13] while most previous research used the maximal SUV in the ventricle.[9 11 19] For the first time, we present marked elevation of glucose metabolism of the right ventricle by calculating the mean SUV_{RV} and mean SUV_{RV}/SUV_{LV} ratio. We have also found good correlations between both methods (online supplementary figure S3).

The main limitation of this study is a relatively small study group and therefore requires future replication on a larger group of patients. However, the study group size is equivalent to similar previous surveys found in this field. Another limitation is that we included patients in clinically stable conditions, so the intrinsic diversity of the group is limited in comparison to the unselected patients seen in everyday practice. Moreover, we were not able to use other PET tracers that could appropriately reflect fatty acid metabolism; therefore, we relied solely on the FDG uptake assessment.

Key messages

What is already known on this subject?

- More advanced changes in pulmonary vascular bed and impaired right ventricle function are associated with increased glucose metabolism of right ventricular myocytes.

What might this study add?

- Better knowledge about significance of cardiac metabolism and its alterations may be an important step in developing potential therapies based on metabolic modulations.

How might this impact on clinical practice?

- Additional positron emission tomography/MRI analysis of patients with pulmonary arterial hypertension may provide new prognostic parameters which could identify the group of patients who potentially might benefit from early therapy escalation, but this hypothesis requires validation in a prospective trial.

To sum up, advanced changes in pulmonary vascular bed and impaired RV function are associated with increased glucose metabolism in the RV as estimated by FDG PET. Combining PET and MRI imaging could provide valuable insight into RV function and provide early signs of clinical deterioration in patients with PAH. Knowledge of the significance of cardiac metabolism and its alterations may be an important step in developing potential therapies based on metabolic modulations. We propose SUV_{RV}/SUV_{LV}, especially in combination with MRI-derived RVEF as a non-invasive parameter associated with RV dysfunction providing valuable prognostic information in PAH. It may depict group of patients in the need of earlier therapy escalation. However, establishing the full potential of observed phenomena in clinical assessment requires further prospective investigation.

Author affiliations
[1]Department of Cardiology, Medical University of Bialystok, Bialystok, Poland
[2]Department of Nuclear Medicine, Medical University of Bialystok, Bialystok, Poland
[3]Laboratory of Molecular Imaging, Medical University of Bialystok, Bialystok, Poland
[4]Department of Nuclear Imaging, Technical University of Munich, Munich, Germany
[5]Department of Cardiology, Wyszynski Hospital, Lublin, Poland
[6]Department of Epidemiology, Cardiovascular Disease Prevention and Health Promotion, National Institute of Cardiology, Warsaw, Poland
[7]Cardiac Magnetic Resonance Unit, Institute of Cardiology, Warsaw, Poland
[8]Department of Radiology, Institute of Cardiology, Warsaw, Poland
[9]Department of Population Medicine and Civilization Diseases Prevention, Medical University of Bialystok, Bialystok, Poland

Acknowledgements The authors would like to thank Ms Cindy Abarca MPH for critical reading of the manuscript and language corrections and to Jacek Jamiolkowski BSc, MD, PhD for statistical consultation.

Contributors RK: took part in all activities related to the conduct of the study and contributed to the study idea, data collection, statistical analysis, discussion and writing of the manuscript. PS, SG: PET results analysis. LM, BM-W, JM: analysis of MRI results. PB, DJ: contributed to the data collection. MH: preparation of MRI procedures and scans. MK, BS, JM, RG, WJM: contributed to data collection and the editing of the manuscript. KAK is the guarantor of the content of the manuscript, oversaw all activities related to the conduct of the study and conceived the study idea, contributed to the statistical analysis, writing and editing of the manuscript.

Funding This work was supported by National Center for Science in Poland ('Preludium' grant 2017/25/N/NZ5/02689 to RK), statutory grants of Medical University of Bialystok and by Leading National Research Center in Bialystok.

Competing interests None declared.

Patient and public involvement Patients and/or the public were not involved in the design, conduct, reporting or dissemination plans of this research.

Patient consent for publication Not required.

Ethics approval The study was approved by the local Bioethics Committee. The study complied with the Declaration of Helsinki. All patients gave written informed consent for participating in the study, including taking and storage of blood samples.

Provenance and peer review Not commissioned; externally peer reviewed.

Data availability statement Data are available on reasonable request.

ORCID iDs
Remigiusz Kazimierczyk http://orcid.org/0000-0003-4517-1498
Karol A Kaminski http://orcid.org/0000-0002-9465-2581

REFERENCES

1 Tuder RM, Abman SH, Braun T, *et al*. Development and pathology of pulmonary hypertension. *J Am Coll Cardiol* 2009;54:S3–9.
2 Vonk-Noordegraaf A, Haddad F, Chin KM, *et al*. Right heart adaptation to pulmonary arterial hypertension: physiology and pathobiology. *J Am Coll Cardiol* 2013;62:D22–33.
3 Benza RL, Miller DP, Gomberg-Maitland M, *et al*. Predicting survival in pulmonary arterial hypertension: insights from the registry to evaluate early and long-term pulmonary arterial hypertension disease management (REVEAL). *Circulation* 2010;122:164–72.
4 Vonk-Noordegraaf A, Westerhof N. Describing right ventricular function. *Eur Respir J* 2013;41:1419–23.
5 Al-Naamani N, Preston IR, Hill NS, *et al*. The prognostic significance of pulmonary arterial capacitance in pulmonary arterial hypertension: single-center experience. *Pulm Circ* 2016;6:608–10.
6 Brittain EL, Pugh ME, Wheeler LA, *et al*. Prostanoids but not oral therapies improve right ventricular function in pulmonary arterial hypertension. *JACC Heart Fail* 2013;1:300–7.
7 Galiè N, Humbert M, Vachiery J-L, *et al*. 2015 ESC/ERS guidelines for the diagnosis and treatment of pulmonary hypertension: the joint Task force for the diagnosis and treatment of pulmonary hypertension of the European Society of cardiology (ESC) and the European respiratory Society (ERS): endorsed by: association for European paediatric and congenital cardiology (AEPC), International Society for heart and lung transplantation (ISHLT). *Eur Heart J* 2016;37:67–119.
8 Lopaschuk GD, Belke DD, Gamble J, *et al*. Regulation of fatty acid oxidation in the mammalian heart in health and disease. *Biochim Biophys Acta* 1994;1213:263–76.
9 Mielniczuk LM, Birnie D, Ziadi MC, *et al*. Relation between right ventricular function and increased right ventricular [18F]fluorodeoxyglucose accumulation in patients with heart failure. *Circ Cardiovasc Imaging* 2011;4:59–66.
10 Ohira H, deKemp R, Pena E, *et al*. Shifts in myocardial fatty acid and glucose metabolism in pulmonary arterial hypertension: a potential mechanism for a maladaptive right ventricular response. *Eur Heart J Cardiovasc Imaging* 2016;17:1424–31.
11 Li W, Wang L, Xiong C-M, *et al*. The prognostic value of 18F-FDG uptake ratio between the right and left ventricles in idiopathic pulmonary arterial hypertension. *Clin Nucl Med* 2015;40:859–63.
12 Delso G, Ziegler S. PET/MRI system design. *Eur J Nucl Med Mol Imaging* 2009;36(Suppl 1):86–92.
13 Rischpler C, Nekolla SG, Kunze KP, *et al*. PET/MRI of the heart. *Semin Nucl Med* 2015;45:234–47.
14 Bax JJ, Veening MA, Visser FC, *et al*. Optimal metabolic conditions during fluorine-18 fluorodeoxyglucose imaging; a comparative study using different protocols. *Eur J Nucl Med* 1997;24:35–41.
15 Martinez-Möller A, Souvatzoglou M, Delso G, *et al*. Tissue classification as a potential approach for attenuation correction in whole-body PET/MRI: evaluation with PET/CT data. *J Nucl Med* 2009;50:520–6.
16 Barger PM, Kelly DP. Fatty acid utilization in the hypertrophied and failing heart: molecular regulatory mechanisms. *Am J Med Sci* 1999;318:36–42.
17 Kantor PF, Robertson MA, Coe JY, *et al*. Volume overload hypertrophy of the newborn heart slows the maturation of enzymes involved in the regulation of fatty acid metabolism. *J Am Coll Cardiol* 1999;33:1724–34.
18 Christe ME, Rodgers RL. Altered glucose and fatty acid oxidation in hearts of the spontaneously hypertensive rat. *J Mol Cell Cardiol* 1994;26:1371–5.
19 Tatebe S, Fukumoto Y, Oikawa-Wakayama M, *et al*. Enhanced [18F]fluorodeoxyglucose accumulation in the right ventricular free wall predicts long-term prognosis of patients with pulmonary hypertension: a preliminary observational study. *Eur Heart J Cardiovasc Imaging* 2014;15:666–72.
20 Oikawa M, Kagaya Y, Otani H, *et al*. Increased [18F]fluorodeoxyglucose accumulation in right ventricular free wall in patients with pulmonary hypertension and the effect of epoprostenol. *J Am Coll Cardiol* 2005;45:1849–55.
21 Yang T, Wang L, Xiong C-M, *et al*. The ratio of (18)F-FDG activity uptake between the right and left ventricle in patients with pulmonary hypertension correlates with the right ventricular function. *Clin Nucl Med* 2014;39:426–30.